Journal of Computers Vol. 31 No. 5, 2020, pp. 290-301
doi:10.3966/199115992020103105022

An Attitude Correction Method of Spinning Bodies Based on Radial Gyroscopes

Shuang-biao Zhang[1*], Xing-cheng Li[2], Jia-qi Yu[3]

[1] School of Information Communication Engineering, Beijing Information Science and Technology University, Beijing 100101, China
zhang_shb@bistu.edu.cn

[2] School of Aerospace Engineering, Beijing Institute of Technology, Beijing 100081, China
xingchli@bit.edu.cn

[3] Beijing Institute of Control and Electronic Technology, Beijing 100038, China
yujq2004@163.com

Received 1 August 2020; Revised 1 September 2020; Accepted 23 September 2020

Abstract. The attitude error originated from the characteristic error of longitudinal gyroscopes mounted in spinning and flying bodies is diverging rapidly and far larger than that originated from the attitude algorithm error. To address this problem, an attitude correction method of spinning bodies based on radial gyroscopes is proposed in this paper. The effect of gyroscope measurement error is deduced based on the angular motion model of spinning bodies. The attitude correction is deduced in detail and the attitude update process is provided as well. The simulations are made considering stochastic error, different spinning speeds and different magnitudes of characteristic error. The results show that the gyroscope measurement error has a big effect on attitude update and the validity of the attitude correction method is verified by the improved accuracy.

Keywords: attitude correction, coning environment, gyroscope measurement error, high spinning speed, spinning bodies

1 Introduction

1.1 Background

Many flying bodies such as rockets projectiles, guided shells and intelligent bullets are designed to have high spinning speed to simplify control system structures, guarantee attack precision and reduce collateral damages. However, this flight mechanism forces the spinning bodies to work under high-spin motion with coning environment due to gyroscopic inertia [1]. Under this kind of complex condition, attitude update as one key point for spinning bodies is affected and generates nonnegligible attitude error for control instruction and navigation update process, which has been a serious problem and an important topic in the control and navigation field for several decades.

The coning environment is regarded as a common motion but a rigorous condition for the induced noncommutativity error of attitude update, and it is useful for optimizing attitude algorithms. The classical coning model is shown as [2]:

$$\boldsymbol{\omega} = \begin{bmatrix} \Omega\left[c(\alpha)-1\right] \\ -\Omega \cdot c(\Omega t) \cdot s(\alpha) \\ -\Omega \cdot s(\Omega t) \cdot s(\alpha) \end{bmatrix}. \tag{1}$$

* Corresponding Author

where $\boldsymbol{\omega}$ is the angular velocity, Ω is the coning angular speed, α is the half coning angle, t is time, $c(\cdot)$ represents $\cos(\cdot)$, $s(\cdot)$ represents $\sin(\cdot)$. This model focuses on the swinging movement of the longitudinal axis without considering self-rotation, so it is more suitable for unspinning bodies such as ships and planes.

But for spinning bodies, self-spin motion is another important factor during updating attitude, because this motion often couples with the coning environment and become a complex motion that the unspinning bodies do not have. Fig. 1 shows the detailed rotation process, x_b represents the longitudinal axis fixed in a spinning body, x, y and z represent three axes of a reference frame, and ω_0 represents the spinning speed. When x_b axis makes self-spin motion with the speed ω_0, it is also making conical motion with the speed Ω around the x axis.

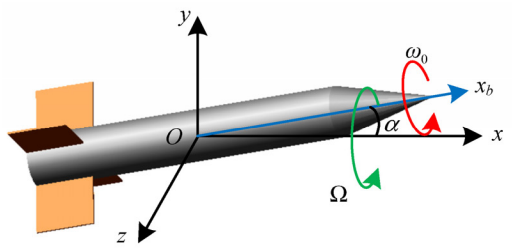

Fig. 1. Complex motion of spinning bodies

So, the complex motion of spinning bodies is modeled by the rotation vector method and it is shown as [3]:

$$\boldsymbol{\omega} = \begin{bmatrix} \Omega\left[c(\alpha)-1\right]+\omega_0 \\ -\Omega \cdot c(\Omega-\omega_0)t \cdot s(\alpha) \\ -\Omega \cdot s(\Omega-\omega_0)t \cdot s(\alpha) \end{bmatrix}. \tag{2}$$

The classical and the complex models are the bases and conditions for the improvement of attitude update.

1.2 Related Work

Attitude algorithms have an important position, and much attention is paid on improving algorithm accuracy. Originally, many researchers are attracted to make deep studies on optimizing and improving attitude algorithms for the interesting classical coning model, shown in (1). The heuristic achievements mainly focus on using rotating vector of subsamples calculation and decreasing attitude drift rate that is recognized as a precision index and is related directly to the number of subsamples [4-6]. Through a series of studies, more subsamples of an algorithm are supposed to have the higher accuracy. Meanwhile, to accommodate real-time performance and updating efficiency for navigation, half-compressed and compressed algorithms are developed and compared to prove the validity [7-8]. To expand the applicability of attitude algorithms, maneuvering conditions are considered to deduce and improve attitude update accuracy by optimizing the high order terms of rotating vector error [9]. The RodFIter method is promising to reconstruct attitude scheme and guarantee precision [10]. Cone attitude and cone attitude algorithm are proved to have higher accuracy than the formal algorithms for the coincidence with the feature of coning motion [1, 11].

All the previous researches are made to reduce attitude error during attitude update, and the algorithm accuracy has been from 10^{-2} up to 10^{-15} degree. However, attitude error still exists during flight, and it diverges rapidly as the spinning speed becomes high. The most probable reason is that attitude error from measurement error of longitudinal gyroscopes mounted on spinning bodies is much bigger than that from attitude algorithms during updating attitude.

Generally, gyroscopes for high spinning speed conditions are based on the MEMS technology, because this kind of gyroscopes is enabled to have a large measurement range by adjusting gyroscope characteristic parameters. The longitudinal gyroscope is often calibrated by simulating flight environment of spinning bodies on a rotation platform, but its measurement error cannot be eliminated thoroughly. On the contrary, the attitude error can be enlarged and accumulated by the real high spinning condition with

attitude update process. Furthermore, the proportional error is a prominent kind of characteristic error, and it plays a main role in angular velocity measurement error. Up to now, the research on this point has not been paid enough attention on, especially considering using the feature of coning motion of spinning bodies. An important fact is that the proportional error of MEMS gyroscopes is determined by the range, and the measurement error of the radial MEMS gyroscopes stays in acceptable extent though the stochastic error existing, due to that the radial gyroscopes have no severe situation as the longitudinal.

Therefore, in this paper, we probe the effect of gyroscope measurement error on the attitude algorithm by using the cone frame under high spinning motion and coning environment, deliver an explorative correction method based on radial gyroscopes to correct cone attitude and examine validity and the application condition of this method.

This paper is organized as follows: Section 2 deduces the effect of gyroscope measurement error on cone attitude. Section 3 provides the cone attitude correction method based on radial gyroscopes. The simulation and analysis are shown in Section 4. In Section 5, this paper is concluded and the future work is presented.

2 Effect of Gyroscope Measurement Error on Attitude Algorithm

2.1 Angular Motion Model

In this paper, we choose the cone frame and the cone attitude to describe the coning motion, because their adequate representation is suited for the angular rotation mechanism of spinning bodies. The rotation relationship between the body frame $Ox_by_bz_b$ and the cone frame $Oxyz$ is shown in Fig. 2, and rotation process is expressed as [1]:

$$Oxyz \xrightarrow[x]{\dot{\delta}_1} Ox'y'z' \xrightarrow[y']{\dot{\delta}_2} Ox'_by'_bz'_b \xrightarrow[x'_b]{\dot{\delta}_3-\dot{\delta}_1} Ox_by_bz_b$$

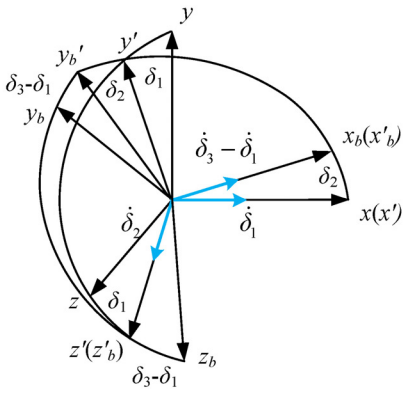

Fig. 2. The rotation process between the body frame and the cone frame

The cone frame is coincident with the inertial frame. The model is expressed as:

$$\begin{bmatrix}\omega_x\\ \omega_y\\ \omega_z\end{bmatrix}=\begin{bmatrix}\dot{\delta}_1\left[c(\delta_2)-1\right]+\dot{\delta}_3\\ -\dot{\delta}_1\cdot c\left(\delta_1-\delta_3\right)\cdot s(\delta_2)-\dot{\delta}_2\cdot s\left(\delta_1-\delta_3\right)\\ -\dot{\delta}_1\cdot s\left(\delta_1-\delta_3\right)\cdot s(\delta_2)+\dot{\delta}_2\cdot c\left(\delta_1-\delta_3\right)\end{bmatrix}. \tag{3}$$

where δ_1, δ_2, δ_3 are the cone attitude and they are the precession angle, the nutation angle and the spin angle in sequence, ω_x, ω_y, ω_z are the elements of angular velocity, $\dot{\delta}_1$, $\dot{\delta}_2$, $\dot{\delta}_3$ are varying speeds of corresponding angles. In the cone frame, the nutation angle δ_2 is equivalent to the half cone angle α, and the procession angular speed $\dot{\delta}_1$ is equivalent to the coning angular speed Ω. According to (3), the cone attitude update equation is written as:

$$\begin{bmatrix}\dot{\delta}_1\\ \dot{\delta}_2\\ \dot{\delta}_3\end{bmatrix}=\begin{bmatrix}0 & -c(\delta_1-\delta_3)/s(\delta_2) & -s(\delta_1-\delta_3)/s(\delta_2)\\ 0 & -s(\delta_1-\delta_3) & c(\delta_1-\delta_3)\\ 1 & -c(\delta_1-\delta_3)\cdot t(\delta_2/2) & -s(\delta_1-\delta_3)\cdot t(\delta_2/2)\end{bmatrix}\begin{bmatrix}\omega_x\\ \omega_y\\ \omega_z\end{bmatrix}. \quad \textbf{(4)}$$

where $t(\cdot)$ represents tan(·).

2.2 Attitude Error by the Effect of Measurement Error

Attitude algorithms focus on attitude update process, but in this paper, we are concerned with the measurement error of triaxial gyroscopes in engineering practice. The actual measurements $\tilde{\omega}$ of triaxial gyroscopes are composed of the ideal value ω and the measurement error $\Delta\omega$, so they are shown as:

$$\tilde{\omega}_x=\omega_x+\Delta\omega_x. \quad \textbf{(5)}$$

$$\tilde{\omega}_y=\omega_y+\Delta\omega_y. \quad \textbf{(6)}$$

$$\tilde{\omega}_z=\omega_z+\Delta\omega_z. \quad \textbf{(7)}$$

The measurement error of triaxial gyroscopes is able to make the cone attitude generate error. So, substituting (5), (6) and (7) to (4), we obtain the cone attitude differential equations with the measurement error and the attitude error:

$$\dot{\delta}_1+\Delta\dot{\delta}_1=-\frac{c(\delta_1+\Delta\delta_1-\delta_3-\Delta\delta_3)}{s(\delta_2-\Delta\delta_2)}\cdot(\omega_y+\Delta\omega_y)-\frac{s(\delta_1+\Delta\delta_1-\delta_3-\Delta\delta_3)}{s(\delta_2-\Delta\delta_2)}\cdot(\omega_z+\Delta\omega_z). \quad \textbf{(8)}$$

$$\dot{\delta}_2+\Delta\dot{\delta}_2=-s(\delta_1+\Delta\delta_1-\delta_3-\Delta\delta_3)\cdot(\omega_y+\Delta\omega_y)+c(\delta_1+\Delta\delta_1-\delta_3-\Delta\delta_3)\cdot(\omega_z+\Delta\omega_z). \quad \textbf{(9)}$$

$$\begin{aligned}\dot{\delta}_3+\Delta\dot{\delta}_3=&(\omega_x+\Delta\omega_x)-c(\delta_1+\Delta\delta_1-\delta_3-\Delta\delta_3)\cdot t\left[(\delta_2+\Delta\delta_2)/2\right]\cdot(\omega_y+\Delta\omega_y)-s(\delta_1+\Delta\delta_1-\delta_3-\Delta\delta_3)\cdot\\ &t\left[(\delta_2+\Delta\delta_2)/2\right]\cdot(\omega_z+\Delta\omega_z)\end{aligned}. \quad \textbf{(10)}$$

where $\Delta\delta_1$, $\Delta\delta_2$, $\Delta\delta_3$ are the cone attitude error, and $\Delta\dot{\delta}_1$, $\Delta\dot{\delta}_2$, $\Delta\dot{\delta}_3$ are the corresponding differential attitude error. Further, from (8) to (10), we obtain:

$$\begin{aligned}\Delta\dot{\delta}_1=&\frac{c(\delta_1-\delta_3)\cdot c(\delta_2)\cdot\Delta\delta_2+s(\delta_1-\delta_3)\cdot(\Delta\delta_1-\Delta\delta_3)}{s(\delta_2)-c(\delta_2)\cdot\Delta\delta_2}\cdot\omega_y+\frac{s(\delta_1-\delta_3)\cdot(\Delta\delta_1-\Delta\delta_3)-c(\delta_1-\delta_3)}{s(\delta_2)-c(\delta_2)\cdot\Delta\delta_2}\cdot\Delta\omega_y\\ &+\frac{s(\delta_1-\delta_3)\cdot c\delta_2\Delta\delta_2+c(\delta_1-\delta_3)\cdot(\Delta\delta_1-\Delta\delta_3)}{s(\delta_2)-c(\delta_2)\Delta\delta_2}\cdot\omega_z+\frac{s(\delta_1-\delta_3)+c(\delta_1-\delta_3)\cdot(\Delta\delta_1-\Delta\delta_3)}{s(\delta_2)c(\Delta\delta_2)-c(\delta_2)\Delta\delta_2}\cdot\Delta\omega_z\end{aligned}. \quad \textbf{(11)}$$

$$\begin{aligned}\Delta\dot{\delta}_2=&-s(\delta_1-\delta_3)\cdot\Delta\omega_y+c(\delta_1-\delta_3)\cdot\Delta\omega_z-c(\delta_1-\delta_3)\cdot(\Delta\delta_1-\Delta\delta_3)\cdot(\omega_{by}+\Delta\omega_y)-s(\delta_1-\delta_3)\cdot(\Delta\delta_1-\Delta\delta_3)\cdot\\ &(\omega_{bz}+\Delta\omega_z)\end{aligned}. \quad \textbf{(12)}$$

$$\begin{aligned}\Delta\dot{\delta}_3=&\Delta\omega_x+c(\delta_1-\delta_3)\cdot t\left(\delta_2/2\right)\cdot\omega_{by}+s(\delta_1-\delta_3)\cdot t\left(\delta_2/2\right)\cdot\omega_{bz}\\ &-c(\delta_1-\delta_3+\Delta\delta_1-\Delta\delta_3)\cdot t\left[(\delta_2+\Delta\delta_2)/2\right]\cdot(\omega_{by}+\Delta\omega_y)-s(\delta_1-\delta_3+\Delta\delta_1-\Delta\delta_3)\cdot t\left[(\delta_2+\Delta\delta_2)/2\right].\\ &\cdot(\omega_{bz}+\Delta\omega_z)\end{aligned} \quad \textbf{(13)}$$

The ideal value and the error value are coupled closely, but it is definite that the cone attitude error is unequal to zero with the non-zero measurement error of triaxial gyroscopes. Decoupling is impractical and unnecessary, and showing the specific results is easy by simulations according to the deduction.

3 Attitude Correction Method Based on Radial Gyroscopes

In this paper, we attempt to use the radial gyroscopes to estimate the roll angle error affected by the longitudinal gyroscope. We assume that the radial gyroscopes have unconspicuous and negligible error during deducing correction process, so the roll angle error is primary.

3.1 Roll Angle Error from Gyroscope Measurement Error

Due to the classical coning environment, we assume the nutation angle is invariable, which makes analyzing more convenient:

$$\begin{bmatrix} \omega_x(t) \\ \omega_y(t) \\ \omega_z(t) \end{bmatrix} = \begin{bmatrix} \dot{\delta}_1(t)\left[c(\delta_2(t))-1\right]+\dot{\delta}_3(t) \\ -\dot{\delta}_1(t)\cdot c\left(\delta_1(t)-\delta_3(t)\right)\cdot s\left(\delta_2(t)\right) \\ -\dot{\delta}_1(t)\cdot s\left(\delta_1(t)-\delta_3(t)\right)\cdot s\left(\delta_2(t)\right) \end{bmatrix}. \tag{14}$$

Using the second and the third elements of (14) at each time, we obtain:

$$\delta_1(t)-\delta_3(t)=\arctan\frac{\omega_z(t)}{\omega_y(t)}. \tag{15}$$

It is clear that the difference value of the precession angle and the roll angle can be calculated when using the radial gyroscope measurement.

Accumulating the value at each time, we obtain:

$$Sum\ 1=\sum_{t=0}^{t=t_N}\delta_1(t)-\delta_3(t)=\sum_{t=0}^{t=t_N}\arctan\frac{\omega_z(t)}{\omega_y(t)}. \tag{16}$$

where t_N is the Nth time.

On the other side, using the second and the third elements of (14) we also obtain:

$$\omega_y^2(t)+\omega_z^2(t)=\dot{\delta}_1^2(t)s^2\left(\delta_2(t)\right). \tag{17}$$

And the following relationships are obtained:

$$\dot{\delta}_1^2(t)=\frac{\omega_y^2(t)+\omega_z^2(t)}{s^2\left(\delta_2(t)\right)}. \tag{18}$$

$$\dot{\delta}_1^2(t)c^2\left(\delta_2(t)\right)=\dot{\delta}_1^2(t)-\left(\omega_y^2(t)+\omega_z^2(t)\right). \tag{19}$$

Then, (19) is derived as:

$$\dot{\delta}_1(t)c\left(\delta_2(t)\right)=\pm\sqrt{\dot{\delta}_1^2(t)-\left(\omega_y^2(t)+\omega_z^2(t)\right)}. \tag{20}$$

Normally, the nutation angle is positive and no greater than π/2, and the precession angular speed is coincident with the roll direction of spinning bodies. So, according to the first element of (14), the sign of (20) can be determined easily by the sign of ω_x.

Meanwhile, the following equation is obtained:

$$\dot{\delta}_3(t)-\dot{\delta}_1(t)=\omega_x(t)-\dot{\delta}_1(t)c\left(\delta_2(t)\right). \tag{21}$$

Considering each parameter value at each time, substituting (18) and (20) to (21) and integrating (21), we obtain:

$$Sum\ 2=\int_{t=0}^{t=t_N}\left(\dot{\delta}_3(\tau)-\dot{\delta}_1(\tau)\right)d\tau=\int_{t=0}^{t=t_N}\left(\omega_x(\tau)\mp\frac{\sqrt{\omega_y^2(\tau)+\omega_z^2(\tau)}}{t(\delta_2)}\right)d\tau. \tag{22}$$

Equation (22) can also be written as:

$$Sum\ 2 = \sum_{t=0}^{t=t_N} \delta_3(t) - \delta_1(t)\,. \tag{23}$$

Obviously, without any error, the relationship of (16) and (23) can be written as:

$$Sum\ 1 = -Sum\ 2\,. \tag{24}$$

Therefore, considering the gyroscope measurement error, we obtain:

$$\sum_{t=0}^{t=t_N} \Delta\varepsilon(t) = Sum\ 1 + Sum\ 2\,. \tag{25}$$

Strictly, the attitude error in (25) is ascribed to the measurement error of triaxial gyroscopes, but the longitudinal gyroscope measurement error is much bigger. The main cone attitude is seen reasonably as the roll angle error. So, this kind of error is approximately considered to result from the longitudinal gyroscope measurement error:

$$\Delta\delta_3(t) = \Delta\varepsilon(t)\,. \tag{26}$$

3.2 Cone Attitude Update Process

Generally, the Runge-Kutta algorithm is used to directly update the cone attitude without measurement error, and the relevant Equations are shown as:

$$y_{i+1} = y_i + \frac{1}{6}(K_1 + 2K_2 + 2K_3 + K_4)\,. \tag{27}$$

$$K_1 = h \cdot f\left(x_i, y_i\right). \tag{28}$$

$$K_2 = h \cdot f\left(x_i + \frac{h}{2}, y_i + \frac{1}{2}K_1\right). \tag{29}$$

$$K_3 = h \cdot f\left(x_i + \frac{h}{2}, y_i + \frac{1}{2}K_2\right). \tag{30}$$

$$K_4 = h \cdot f\left(x_i + h, y_i + K_3\right). \tag{31}$$

where $f(\cdot)$ represents the differential equation, y_i represents integral function, x_i represents variable, h represents update time, K_i is the coefficients, and i represents 1, 2, 3, 4.

Since the cone attitude error is propagated from gyroscopes, the update process should be improved to restrain the effect based on the Runge-Kutta algorithm. The detailed attitude update process is shown in Fig. 3. At the beginning, angular velocity data are sampled from triaxial gyroscopes by fixed sample time, and then they are putted into data process. At the same time, the cone attitude is initialized. On one side, angular velocity data are used directly into the cone attitude differential equation to update cone attitude by Runge-Kutta, which would generate attitude error. On the other side, angular velocity data are also used to estimate attitude error. Then, the attitude correction is to do subtraction with the results from both sides during each update period. Through iteration based on the Fig. 3, the cone attitude can be corrected.

4 Simulation and Analysis

In this section, we design and make simulations to show the effect of gyroscopes error on the attitude update, and then prove the validity of the attitude correction method.

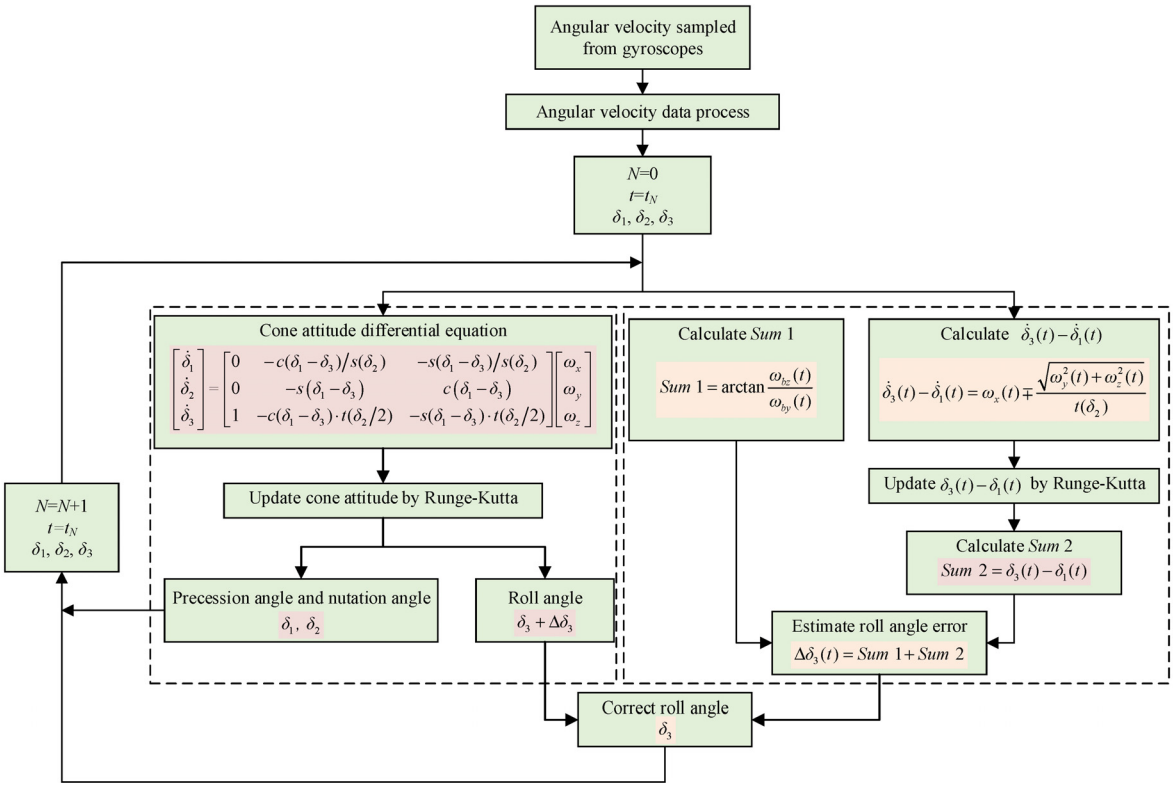

Fig. 3. The detailed attitude update process

4.1 Effect of Gyroscopes Error on Attitude Update

We classify the error type into the stochastic error and the measurement error, which could provide clear comparison to show explain the detail effect. The stochastic error exists all the time in engineering practice, and it should be considered to check the effect on the previous attitude algorithm. The accuracy of the attitude algorithm that is proven to be 10^{-15} degree in [8] would not change with the cone attitude.

Firstly, we design the same Gaussian white noise as the stochastic error for triaxial gyroscopes without other type error, which is easy to examine the cone attitude error. Meanwhile, we design the coning environment is static with the simulation condition shown in Table 1. The half angle 5° and coning angular speed 180°/s and the spinning speeds are 360°/s, 720°/s, 1440°/s, and 2880°/s.

Table 1. The simulation condition for only stochastic error

Simulation	α (°)	Ω (°/s)	ω_0 (°/s)
S_1	5	180	360
S_2	5	180	720
S_3	5	180	1440
S_4	5	180	2880

The stochastic error effect is shown in Fig. 4. Although the precession angle error and the nutation angle error are affected to vibrate, the roll angle still appear stochastically. The maximums of attitude error by the stochastic error effect are recoded in Table 2, and they are no greater than one degree during 60s. This means the stochastic error tends to lead to vibration error but has no enough effect on the attitude algorithm to diverge with time rapidly.

Then, we add the characteristic error to the stochastic error as the measurement error of triaxial gyroscopes. This kind of characteristic error tend to appear linearly varying with triaxial rotation condition, and the calibration of different axial gyroscopes cannot restrain the error thoroughly. So, to show the effect of the proportional error clearly, we assure firstly that the triaxial gyroscopes have the same proportion 0.001%, and examine the cone attitude error under different simulation conditions shown in Table 3.

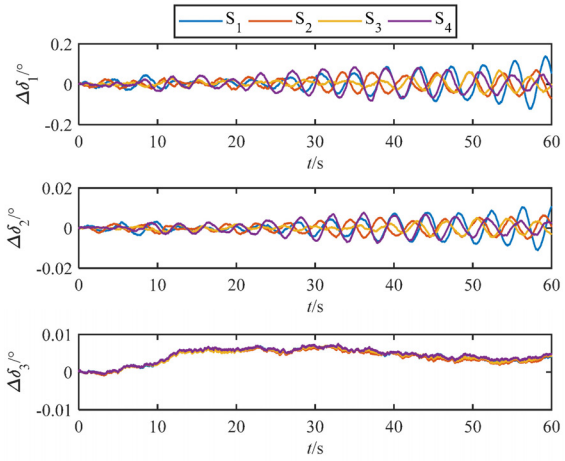

Fig. 4. Cone attitude error affected by the stochastic error

Table 2. The maximums of attitude error by the stochastic error effect

Simulation	$\Delta\delta_1$ (°)	$\Delta\delta_2$ (°)	$\Delta\delta_3$ (°)
S_1	0.1383	0.01113	0.007326
S_2	0.07125	0.006342	0.006671
S_3	0.03745	0.003278	0.007044
S_4	0.03141	0.003591	0.007526

Table 3. The simulation condition for stochastic error and constant measurement error

Simulation	α (°)	Ω(°/s)	ω_0 (°/s)	Proportional error (%)
S_5	5	180	360	0.001
S_6	5	180	720	0.001
S_7	5	180	1440	0.001
S_8	5	180	2880	0.001

The results are shown in Fig. 5, and the precession angle and the roll angle are affected badly and diverge rapidly with time though the nutation angle affected slightly. The maximums of attitude error by the characteristic error effect are recoded in Table 4. Attitude error increases manyfold, and the diverging rate is determined by the increasing ratio of the spinning speeds. The results show apparently that the characteristic error leads the attitude algorithm to generate divergence error.

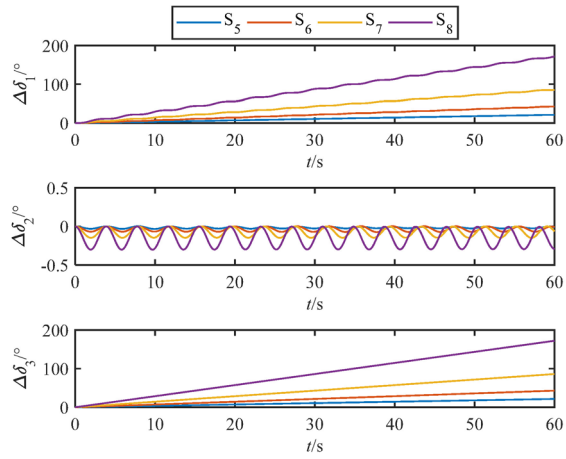

Fig. 5. Cone attitude affected by the characteristic error

Table 4. The maximums of attitude error by the characteristic error effect

Simulation	$\Delta\delta_1$ (°)	$\Delta\delta_2$ (°)	$\Delta\delta_3$ (°)
S_5	42.84	-0.06836	43.06
S_6	85.36	-0.1360	86.12
S_7	216.5	-0.3367	215.3
S_8	427.1	-0.6351	430.7

To examine further how the characteristic error affects, we design the different proportion error for the triaxial gyroscopes, 0.001%, 0.002%, 0.005% and 0.01%. The flight environment is the spinning speed 1440°/s, the half angle α 5° and the coning angular speed Ω 180°/s.

Table 5. The simulation condition for stochastic error and different measurement error

Simulation	α(°)	Ω(°/s)	ω_0 (°/s)	Proportional error (%)
S_9	5	180	1440	0.001
S_{10}	5	180	1440	0.002
S_{11}	5	180	1440	0.005
S_{12}	5	180	1440	0.01

The results are shown in Fig. 6, and the cone attitude error diverges with time much more fiercely. The maximums of attitude error by the different magnitudes of characteristic error are recoded in Table 6, and the attitude error has increased up to 861.4° during 60s. This proves the diverging rate is multiplied as the proportion error enlarges. Comparing with the simulation results above, it is apparent that the characteristic error has a big effect on the attitude algorithm.

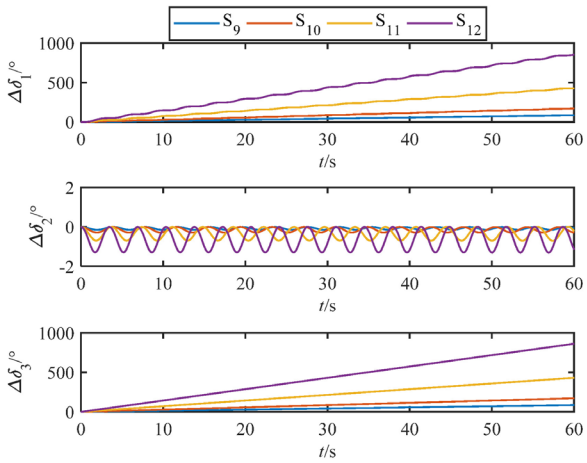

Fig. 6. Cone attitude error affected by the different magnitudes of characteristic error

Table 6. The maximums of attitude error by the different magnitudes of characteristic error

Simulation	$\Delta\delta_1$ (°)	$\Delta\delta_2$ (°)	$\Delta\delta_3$ (°)
S_9	85.23	-0.1487	86.10
S_{10}	171.9	-0.2868	172.2
S_{11}	426.6	-0.6941	430.6
S_{12}	855.3	-1.305	861.4

4.2 Validity of the Attitude Correction Method

To verify the validity of the correction method proposed in this paper, we choose the condition in Table 3 firstly. The results are shown in Fig. 7 and the maximums of attitude error by the correction method for different spinning speeds are shown in Table 7. The cone attitude error overlaps together during 60s and it has been restrained from 430.7° down to 7.512° by comparing with Table 4 though it is still diverging

with time in Fig. 7. Moreover, the attitude error is not affected to diverge by the spinning speed. This means the attitude correction method restrains the attitude error, and the accuracy has been improved 98.3%. The reason for the remaining error is due to the measurement error of radial gyroscopes.

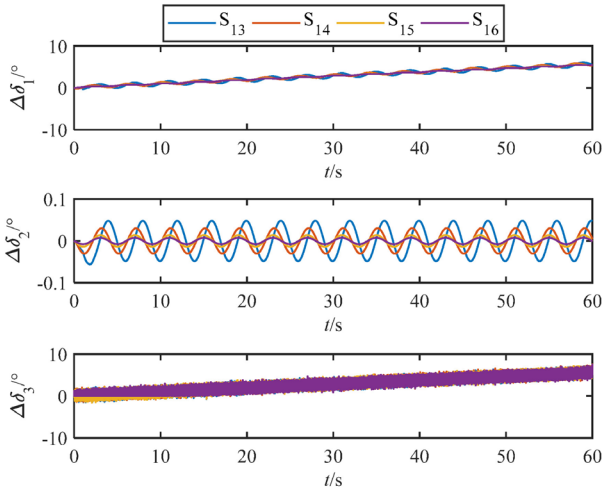

Fig. 7. The validity of the correction method for different spinning speeds

Table 7. The maximums of attitude error by the correction method for different spinning speeds

Simulation	$\Delta\delta_1$ (°)	$\Delta\delta_2$ (°)	$\Delta\delta_3$ (°)
S_{13}	6.6066	0.04825	7.543
S_{14}	5.84	0.03029	7.596
S_{15}	5.613	0.01371	7.559
S_{16}	5.481	0.007457	7.512

Then, we choose the condition in Table 5 to examine the validity of the method for the different magnitudes of the characteristic error. The results are shown in Fig. 8, and the maximums of attitude error are recorded in Table 8. The cone attitude error is diverging linearly with time but has been restrained from 861.4° down to 56.14° comparing with the result in Table 6. The diverging rate also decreases less than the increasing ratio of spinning speeds, and the accuracy has been improved 93.5%. Comparing with Table 7, the characteristic error is found more influential than the spinning speeds.

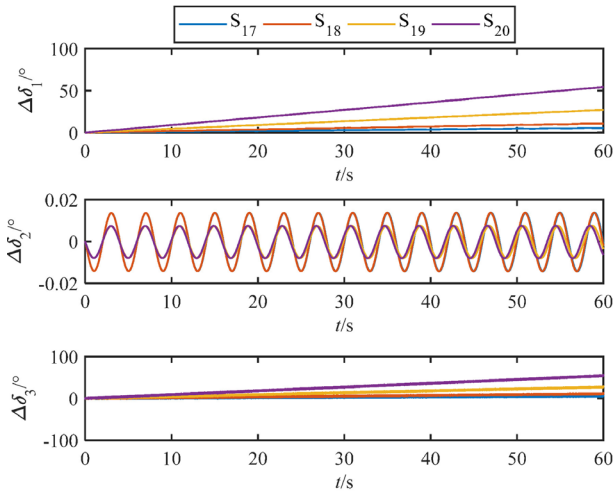

Fig. 8. The validity of the correction method for different magnitudes of characteristic error

Table 8. The maximums of attitude error by the correction method for different magnitudes of characteristic error

Simulation	$\Delta\delta_1$ (°)	$\Delta\delta_2$ (°)	$\Delta\delta_3$ (°)
S_{17}	5.84	0.03029	7.596
S_{18}	10.86	0.01371	10.49
S_{19}	27.14	0.006567	26.64
S_{20}	54.15	0.007495	56.14

5 Conclusion

In order to address the effect of gyroscope measurement error on attitude algorithms for spinning bodies under coning environment, this paper proposes an attitude correction method based on radial gyroscopes. The cone frame and the cone attitude are used to model the angular motion of spinning bodies, and the effect equations are deduced by considering the measurement error. Based on the angular model of spinning bodies, the measurement of radial gyroscopes is used to deduce the attitude correction and the detailed attitude update process is provided as well. The simulations are made and the results show that the measurement error has a huge effect than the stochastic error and the spinning speed of spinning bodies, which is able to lead the attitude algorithm to generate diverging error that is far more than the error of previous attitude algorithms. Meanwhile, the validity of attitude correction method is verified, and the accuracy is improved greatly. This research aims to highlight that the gyroscope proportion error is an more important factor of attitude update error, the performance improvement and the application of appropriate gyroscopes in different spinning speeds of spinning bodies, and this paper could also provide a promising way for data preprocessing of gyroscopes.

In the future work, we will consider more complex flight environment and focus on estimating the whole characteristic error of triaxial gyroscopes in real time.

Acknowledgments

This study is financially supported in part by the National Natural Science Foundation of China under Grant 61771059, in part by the Innovation Project of Beijing Municipal Education Commission under Grant KM201911232013, and in part by the Key Cultivation Project of Beijing Information Science and Technology University under Grant 5211910952.

Reference

[1] S. Zhang, Z. Su, X. Li, Real-time angular motion decoupling and attitude updating method of spinning bodies assisted by satellite navigation data, IEEE Access 7(2019)184340-184350.

[2] J.E. Bortz, A new mathematical formulation for strapdown inertial navigation, IEEE Transactions on Aerospace and Electronic Systems 7(1)(1971) 61-66.

[3] M. Wang, W. Wu, J. Wang, X. Pan, High-order attitude compensation in coning and rotation coexisting environment, IEEE Transactions on Aerospace and Electronic Systems 51(2)(2015) 1178-1190.

[4] J.G. Lee, Y.J. Yoon, J.G. Mark, D.A. Tazartes, Extension of strapdown attitude algorithm for high-frequency base motion, Journal of Guidance, Control, and Dynamics 13(4)(1990) 738-743.

[5] M.B. Ignagni, Efficient class of optimized coning compensation algorithms, Journal of Guidance, Control, and Dynamics 19(2)(1996) 424-429.

[6] P.G. Savage, Explicit frequency-shaped coning algorithms for pseudo-coning environments, Journal of Guidance Control & Dynamics 34(2)(2015) 774-782.

[7] C. Tang, L. Chen, J. Chen, Efficient coning algorithm design from a bilateral structure, Aerospace Science & Technology 79(2018) 48-57.

[8] R.B. Miller, A new strapdown attitude algorithm, Journal of Guidance, Control, and Dynamics 6(4)(1983) 287-291.

[9] J. Pan, G. Wang, Y. Zhang, L. Zhang, S. Fan, D. Xu, An improved attitude compensation algorithm in high dynamic environment, IEEE Sensors Journal 20(1)(2020) 306-317.

[10] Y. Wu, RodFIter: attitude reconstruction from inertial measurement by functional iteration, IEEE Transactions on Aerospace and Electronic Systems 54(5)(2018) 2131-2142.

[11] S. Zhang, X. Li, Z. Su, Cone algorithm of spinning vehicles under dynamic coning environment, International Journal of Aerospace Engineering 1(2015) 1-10.